Mode of Interaction of Hydrophobic Amphiphilic α-Helical Peptide/ Dipalmitoylphosphatidylcholine with Phosphatidylglycerol or Palmitic Acid at the Air−Water Interface

Hiromichi Nakahara,[†] Sannamu Lee,[‡] Gohsuke Sugihara,[‡] and Osamu Shibata*,[†]

Division of Biointerfacial Science, Graduate School of Pharmaceutical Sciences, Kyushu University, 3-1-1 Maidashi, Higashi-ku, Fukuoka 812-8582, Japan, and Department of Chemistry, Faculty of Science, Fukuoka University, 8-19-1 Nanakuma, Johnan-ku, Fukuoka 814-0180, Japan

Received January 20, 2006. In Final Form: April 10, 2006

Surface pressure (π)−, surface potential (ΔV)−, dipole moment ($\mu_\perp$)−area (A) isotherms and morphological behavior at the air−water interface were obtained for multicomponent monolayers of two different systems for dipalmitoylphosphatidylcholine (DPPC)/egg-phosphatidylglycerol (PG) (= 68:22, by weight)/Hel 13-5 and DPPC/palmitic acid (PA) (= 90:9, by weight)/Hel 13-5 (Hel 13-5 is a newly designed 18-mer amphiphilic α-helical peptide with 13 hydrophobic and 5 hydrophilic amino acid residues). The phase behavior of these model systems was investigated on a subsolution of 0.02 M tris(hydroxymethyl)aminomethane (Tris) buffer (pH 8.4) with 0.13 M NaCl at 298.2 K by employing the Wilhelmy method, the ionizing electrode method, and fluorescence microscopy. Especially, the present study focuses on the interfacial effect of the addition of Hel 13-5 on two binary systems, DPPC/egg-PG and DPPC/PA monolayers, as the substitute for pulmonary surfactant proteins, and on the respective roles of PG and PA for the monolayers in the three-component systems. Constant kink points (∼42 mN m^{-1}) clearly appear on the $\pi-A$ isotherms, independent of the compositions in the ternary systems, which corresponds to the Hel 13-5 collapse pressure similar to that of SP-B and SP-C as functions in multicomponent monolayers. This implies that Hel 13-5 is squeezed out of ternary monolayers above ∼42 mN m^{-1}, resulting in two- to three-dimensional phase transformation. Furthermore, Langmuir isotherms clearly show that Hel 13-5 with egg-PG is squeezed out of the DPPC/egg-PG/Hel 13-5 system, whereas only Hel 13-5 is squeezed out of the DPPC/PA/Hel 13-5 system. Cyclic compression and expansion isotherms of these systems were carried out to confirm the spreading and respreading capacities. In addition, the interfacial behavior of the ternary mixtures has been analyzed by the additivity rule. Morphological examinations and comparisons have verified the interactions of Hel 13-5 with the representative miscible mixture (DPPC/PA system) by fluorescence microscopy. Consequently, distinct morphological variations corresponding to the squeeze-out behavior are observed as a fluorescent contrast recovery. Herein, a new mechanism of the refluorescent phenomenon is proposed by varying the surface composition of Hel 13-5.

Introduction

Surface-active materials lining up at the air−alveolar fluid interface in mammalian lungs or pulmonary surfactants (PS) play an important role in vital physiological processes such as respiratory movement. First, at the interface, PS reduces surface tension to minimize the work of breathing and to prevent alveolar collapses in expiratory movements.[1] Second, PS rapidly adsorbs and spreads to the interface.[2] PS is a mixture of lipids (∼90 wt %) and proteins (∼10 wt %) synthesized and secreted into the alveolar fluid by alveolar type II epithelial cells. The material consists mainly of phosphatidylcholines (especially, dipalmitoylphosphatidylcholine (DPPC), ∼50 wt %) and smaller but significant amounts of phosphatidylglycerol (PG), palmitic acid (PA), and four proteins (SP-A, -B, -C, and -D).[3−6]

DPPC has properties of lowering surface tension near zero in the multilayer state. However, its rigidity at physiological conditions causes it to adsorb slowly from the alveolar fluid and to respread poorly from multiple materials.[7] The unsaturated and anionic PG is thought to help DPPC molecules adsorb and respread rapidly. PA presents in a relatively low amount in comparison with DPPC, but it has been referred to as a very important additive for the proper functioning of both natural and synthetic PS replacement formulations. The addition of ∼10 wt % PA to natural PS extracts obtained from animal sources has induced a significant improvement in their properties both in vitro and in vivo.[8,9]

Besides lipids, it has been found that four proteins (SP-A, -B, -C, and -D) are associated with PS in many cases.[10,11] SP-A and SP-D of hydrophilic proteins have demonstrated that they play an important role in the first-line defenses against inhaled pathogens[12] and in the storage and transport of PS.[13,14] On the

* Corresponding author. Address: Division of Biointerfacial Science, Graduate School of Pharmaceutical Sciences, Kyushu University, 3-1-1 Maidashi, Higashi-ku, Fukuoka 812-8582, Japan. Tel/Fax: +81-92(642) 6669. E-mail: shibata@phar.kyushu-u.ac.jp. Website: http://210.233.60.66/∼kaimen/.

† Kyushu University.

‡ Fukuoka University.

(1) Schürch, S.; Goerke, J.; Clements, J. A. *Proc. Natl. Acad. Sci. U.S.A.* **1976**, *73*, 332−338.

(2) Bastacky, J.; Lee, C. Y.; Goerke, J.; Koushafar, H.; Yager, D.; Speed, T. P.; Chen, Y.; Clements, J. A. *J. Appl. Physiol.* **1995**, *79*, 1615−1628.

(3) Krüger, P.; Baatz, J. E.; Dluhy, R. A.; Lösche, M. *Biophys. Chem.* **2002**, *99*, 209−228.

(4) Postle, A. D.; Heeley, E. L.; Wilton, D. C. *Comp. Biochem. Physiol., A* **2001**, *129*, 65−73.

(5) Veldhuizen, R.; Nag, K.; Orgeig, S.; Possmayer, F. *Biochim. Biophys. Acta* **1998**, *1408*, 90−108.

(6) Yu, S.-H.; Possmayer, F. *J. Lipid Res.* **2003**, *44*, 621−629.

(7) Fleming, B.; Keough, K. M. W. *Chem. Phys. Lipids* **1988**, *49*, 81−86.

(8) Cockshutt, A.; Absolom, D.; Possmayer, F. *Biochim. Biophys. Acta* **1991**, *1085*, 248−256.

(9) Gorree, G.; Egberts, J.; Bakker, G.; Beintema, A.; Top, M. *Biochim. Biophys. Acta* **1991**, *1086*, 209−216.

(10) Hawgood, S.; Shiffer, K. *Annu. Rev. Physiol.* **1991**, *53*, 375−394.

(11) Johansson, J.; Curstedt, T. *Eur. J. Biochem.* **1997**, *244*, 675−693.

(12) Miyamura, K.; Leigh, L. E. A.; Lu, J.; Hopkins, J.; Lopez-Bernal, A.; Reid, K. B. M. *Biochem. J.* **1994**, *300*, 237−242.

(13) Goerke, J. *Biochim. Biophys. Acta* **1974**, *344*, 241−261.

10.1021/la060194h CCC: $33.50
Published on Web 05/18/2006

contrary, SP-B and SP-C are hydrophobic proteins that dominate the surface activity of PS. They considerably promote the adsorption of PS from the hypophase to the monolayer at the air−water interface. Furthermore, they trigger a reversible exclusion of fluid materials from the multicomponent monolayers when they are compressed beyond their collapse pressures.[15−17] In general, this behavior has been known as the "squeeze-out" phenomenon, proposing that unsaturated lipids and proteins in PS are selectively and reversibly removed or squeezed out of the multicomponent monolayer upon overcompression, and leading to DPPC-rich monolayers at the interface.[18,19] It has been suggested that the squeezed-out materials form and occupy a "surface-associated reservoir" at the adjacent interface.[20−22] This squeeze-out phenomenon is indispensable for PS function. However, its mechanism has not been made clear yet.

A deficiency of PS (mainly, inborn lacks) has been shown to cause neonatal respiratory distress syndrome (NRDS) in premature infants.[23] In a related distress for adults, an acquired inactivation of PS is likely to set up adult respiratory distress syndrome (ARDS). So far, a common treatment of NRDS is the surfactant replacement therapy in which exogenous surfactant preparations are administered to NRDS infants. These medicines can be roughly divided into two types. The first is the natural-based source obtained from animals. This preparation is mostly used in clinical cases. However, it has dangers of animal infections such as bovine spongiform encephalopathy (BSE) and so on. In addition, it has a high-cost problem due to the complexity of its extraction and refinement. The second is a synthetic type made from synthetic surfactants with or without proteins. The latter had previously been studied as a substitute for natural types, and then some medicines (Exosurf, ALEC, etc.) were developed.[24,25] Although these medicines can be used at low cost, they do not have a sufficient beneficial effect because they contain no proteins. Thus, the former is currently under consideration and development. In particular, this preparation contains protein analogues or peptides that possess shorter amino acid residues than native SP-B and -C, with the aim of cost reduction.[26−29] Although a few medicines containing new protein analogues have been developed,[28,30] no replacement surfactant has been found comparable to the complete native surfactant with SP-B and -C. Therefore, the development of such synthetic-type medicine is considerably desired.

The authors have investigated the potential use of Hel 13-5 as a PS protein analogue using Langmuir monolayer techniques that simulate pulmonary breathing movement well. The Hel 13-5 peptide was synthesized to mimic the structural balance and function of native SP-B, and was found to form membrane structures resembling cellular organelles such as the Golgi apparatus.[31−34] Constant kink points in response to the collapse pressures of the Hel 13-5 monolayer (∼42 mN m^{-1}) clearly appeared in the surface pressure−area (π−A) isotherms, independent of the compositions in the multicomponent system, where Hel 13-5 was squeezed out of the binary DPPC/Hel 13-5 systems toward an aqueous subphase such as the surface-associated reservoir.[35,36]

In the present study, the Langmuir monolayer behavior of Hel 13-5 and binary DPPC/egg-PG (= 68/22, by weight) or DPPC/PA (= 90/9, by weight) mixtures has been investigated to verify their capabilities as replacement PS. In particular, the study reported here focuses on clarifying each role of PG and PA in the presence of both DPPC and Hel 13-5 monolayers. The lipid mixture (DPPC/PG/PA = 68:22:9, by weight) has shown compositions most similar to alveolar membranes.[28,37,38] Thus, binary lipid systems (DPPC/egg-PG and DPPC/PA) with a fixed ratio were selected here. As far as we know, there is no paper that presents information on PA effects in ternary DPPC/PA/protein (or peptide) systems. Therefore, these examinations are very important for understanding the respective roles of PG and PA components in the PS system and provide evaluative information for synthetic PS preparations.

Materials and Methods

Materials. Hel 13-5 (MW: 2203 Da) was synthesized as described previously.[31] DPPC (purity > 99%) and egg-PG (purity > 99%) were obtained from Avanti Polar Lipids, Inc. (Alabaster, AL). Egg-PG was supplied as its sodium salt. PA (purity > 99%) was purchased from Sigma (St. Louis, MO). 3,6-bis(diethylamino)-9-(2-octadecyloxycarbonyl) phenyl chloride (R18) was obtained from Molecular Probes as a fluorescent probe. These lipids were used without further purification or characterization. *n*-Hexane and ethanol (specially prepared reagent, 99.5%) used as spreading solvents came from Merck (Uvasol) and Nacalai Tesque, respectively. Tris(hydroxymethyl)aminomethane (Tris) and acetic acid (HAc) for the preparation of a subphase were purchased from Nacalai Tesque and supplied as a guaranteed reagent. Sodium chloride (Nacalai Tesque) was roasted at 1023 K for 24 h to remove all surface-active organic impurities.

We used two model surfactant lipids with fixed ratios: DPPC/egg-PG (= 68:22, by weight) and DPPC/PA (= 90:9, by weight) mixtures. The subphase was kept at 0.02 M Tris buffer (pH 8.4) with 0.13 M NaCl solution throughout the experiment to approach the

(14) Voorhout, W. F.; Veenendaal, T.; Haagsman, H. P.; Verkleij, A. J.; van Golde, L. M. G.; Geuze, H. J. *J. Histochem. Cytochem.* **1991**, *39*, 1331−1336.
(15) Taneva, S.; Keough, K. M. W. *Biophys. J.* **1994**, *66*, 1137−1148.
(16) Taneva, S.; Keough, K. M. W. *Biophys. J.* **1994**, *66*, 1149−1157.
(17) Taneva, S.; Keough, K. M. W. *Biophys. J.* **1994**, *66*, 1158−1166.
(18) Lipp, M. M.; Lee, K. Y. C.; Takamoto, D. Y.; Zasadzinski, J. A.; Waring, A. J. *Phys. Rev. Lett.* **1998**, *81*, 1650−1653.
(19) Nahmen, A. V.; Schenk, M.; Sieber, M.; Amrein, M. *Biophys. J.* **1997**, *72*, 463−469.
(20) Ding, J.; Doudevski, I.; Warriner, H. E.; Alig, T.; Zasadzinski, J. A. *Langmuir* **2003**, *19*, 1539−1550.
(21) Schürch, S.; Green, F. H. Y.; Bachofen, H. *Biochim. Biophys. Acta* **1998**, *1408*, 180−202.
(22) Takamoto, D. Y.; Lipp, M. M.; Nahmen, A. V.; Lee, K. Y. C.; Waring, A. J.; Zasadzinski, J. A. *Biophys. J.* **2001**, *81*, 153−169.
(23) Avery, M. E.; Mead, J. *Am. J. Dis. Child.* **1959**, *97*, 517−526.
(24) Kirkness, J. P.; Eastwood, P. R.; Szollosi, I.; Platt, P. R.; Wheatley, J. R.; Amis, T. C.; Hillman, D. R. *J. Appl. Physiol.* **2003**, *95*, 357−363.
(25) Kirkness, J. P.; Madronio, M.; Stavrinou, R.; Wheatley, J. R.; Amis, T. C. *J. Appl. Physiol.* **2003**, *95*, 1761−1766.
(26) Cai, P.; Flach, C. R.; Mendelsohn, R. *Biochemistry* **2003**, *42*, 9446−9452.
(27) Cochrane, C. G.; Revak, S. D.; Merritt, T. A.; Heldt, G. P.; Hallman, M.; Cunningham, M. D.; Easa, D.; Pramanik, A.; Edwards, D. K.; Alberts, M. S. *Am. J. Respir. Crit. Care Med.* **1996**, *153*, 404−410.
(28) Ma, J.; Koppenol, S.; Yu, H,; Zografi, G. *Biophys. J.* **1998**, *74*, 1899−1907.
(29) Revak, S. D.; Merritt, T. A.; Cochrane, C. G.; Heldt, G. P.; Alberts, M. S.; Anderson, D. W.; Kheiter, A. *Pediat. Res.* **1996**, *39*, 715−724.
(30) Veldhuizen, E. J. A.; Waring, A. J.; Walther, F. J.; Batenburg, J. J.; van Golde, L. M. G.; Haagsman, H. P. *Biophys. J.* **2000**, *79*, 377−384.
(31) Kiyota, T.; Lee, S.; Sugihara, G. *Biochemistry* **1996**, *35*, 13196−13204.
(32) Furuya, T.; Kiyota, T.; Lee, S.; Inoue, T.; Sugihara, G.; Logvinova, A.; Goldsmith, P.; Ellerby, H. P. *Biophys. J.* **2003**, *84*, 1950−1959.
(33) Kitamura, A.; Kiyota, T.; Tomohiro, M.; Umeda, A.; Lee, S.; Inoue, T.; Sugihara, G. *Biophys. J.* **1999**, *76*, 1457−1468.
(34) Lee, S.; Furuya, T.; Kiyota, T.; Takami, N.; Murata, K.; Niidome, Y.; Bredesen, D. E.; Ellerby, H. M.; Sugihara, G. *J. Biol. Chem.* **2001**, *276*, 41224−41228.
(35) Nakahara, H.; Nakamura, S.; Lee, S.; Sugihara, G.; Shibata, O. *Colloids Surf., A* **2005**, *270*−*271*, 52−60.
(36) Nakahara, H.; Nakamura, S.; Hiranita, T.; Kawasaki, H.; Lee, S.; Sugihara, G.; Shibata, O. *Langmuir* **2006**, *22*, 1182−1192.
(37) Gustafsson, M.; Vandenbussche, G.; Curstedt, T.; Ruysschaert, J. M.; Johansson, J. *FEBS Lett.* **1996**, *384*, 185−188.
(38) Gustafsson, M.; Palmblad, M.; Curstedt, T.; Johansson, J.; Schürch, S. *Biochim. Biophys. Acta* **2000**, *1466*, 169−178.

conditions in a living body, conditions supported by many researchers.[28,39−41]

Methods. *Surface Pressure−Area Isotherms.* The surface pressure (π) of monolayers was measured using an automated homemade Wilhelmy balance, which was the same as that used in previous studies.[42−44] The surface pressure balance (Mettler Toledo, AG-64) had a resolution of 0.01 mN m^{-1}. The pressure-measuring system was equipped with a filter paper (Whatman 541, periphery = 4 cm). The trough was made from Teflon-coated brass (area = 750 cm^2), and Teflon-made barriers (both hydrophobic and lipophobic) were used in this study. The compression process for typical phospholipids such as DPPC could reach pressures close to 70 mN m^{-1} without leakage of materials by using hydrophilic barriers; however, an entire Teflon-made system makes it possible to prevent the adsorption of materials onto barriers and to elucidate quantitative analyses up to the monolayer collapse states of phospholipids exactly. The surface potential measurement also supports this behavior.[36]

The $\pi-A$ isotherms were recorded at 298.2 ± 0.05 K. Stock solutions of DPPC (1.35 mM), egg-PG (0.68 mM), and PA (1.35 mM) were prepared in *n*-hexane/ethanol (9:1 v/v), and those of Hel 13-5 were made in *n*-hexane/ethanol (4.5:5.5 v/v). The spreading solvents were allowed to evaporate for 15 min prior to compression. The monolayer was compressed at a speed of <0.45 nm^2 $molecule^{-1}$ min^{-1}. In cycling experiments, the films were compressed and expanded alternately through five cycles at a rate of ∼0.1 nm^2 $molecule^{-1}$ min^{-1}. The standard deviations for the area and surface pressure measurements were ∼0.01 nm^2 and ∼0.1 mN m^{-1}, respectively. The subphase pH was controlled with 0.02 M Tris buffer and 0.13 M NaCl and was adjusted to 8.4 with an adequate amount of HAc. Throughout these studies, the water used was thrice-distilled (surface tension = 72.7 mN m^{-1} at 293.2 K, and electrical resistivity = 18 MΩ cm).

Surface Potential Measurements. The surface potential (ΔV) was simultaneously recorded with pressure while the monolayer was compressed. It was monitored by using an ionizing ^{241}Am electrode at 1−2 mm above the interface while a reference electrode was dipped in the subphase. The standard deviation for the surface potential was ∼5 mV. The other experimental conditions were the same as those described in previous papers.[42−44]

Fluorescence Microscopy (FM). Fluorescence microscope (U.S.I. System BM-1000) observation and compression isotherm measurement were carried out simultaneously. A spreading solution of the surfactants was prepared as a mixed solution doped with 1 mol % of a fluorescence probe (R18). A 300 W xenon lamp (XL 300, Pneum) was used for the excitation of the FM probes. Excitation and emission wavelengths were selected by an appropriate beam splitter/filter combination (Mitutoyo band path filter = 546 nm, Olympus cut filter = 590 nm). The monolayer was observed by using a 20-fold magnification of long-distance objective lens (Mitutoyo, f = 200/focal length = 20 mm). Fluorescent micrographs were recorded with a video camera (757 JAI ICCD camera, Copenhagen, Denmark) connected to the microscope directly into computer memory via an on-line image processor (Vaio PCV−R53 Sony, Video Capture Soft). The entire optical setup was placed on an active vibration isolation unit (model-AY-1812, Visolator, MeiritsuSeiki, Yokohama, Japan). Image processing and analysis were carried out by using the software Scion Image Beta 4.02 for Windows (Scion Corp., Frederick, MD). The total amount of condensed domains (or liquid-condensed (LC) domains) was calculated and expressed as a percentage per frame by dividing the respective frame into black and white regions.

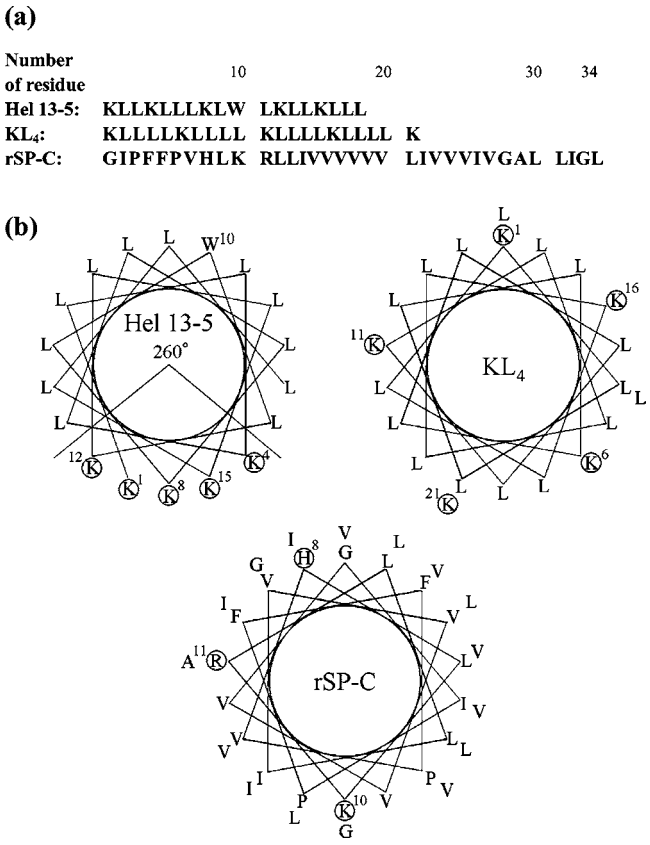

Figure 1. (a) Amino acid sequences of synthetic peptides (Hel 13-5, KL_4, and rSP-C) mimicking native SP-B and SP-C. (b) Helical wheel representations of these peptides. The abbreviations with and without open cycles denote hydrophilic and hydrophobic amino acids, respectively.

Results

Properties of Model Surfactant Lipids and Pure Hel 13-5. The amphiphilic α-helical peptide (Hel 13-5) consists of 13 hydrophobic residues (12 Leu and 1 Trp) and 5 hydrophilic residues (5 Lys). The primary structures of Hel 13-5, KL_4 (21 amino acid peptides) and rSP-C (34 amino acid peptides), are shown in Figure 1a. KL_4 peptides have been used as an element in synthetic-type RDS medicines (or Surfaxin) to mimic the native SP-B,[26,28,37] whereas rSP-C peptides are in clinical trials (Phase III) as that in Venticute and are based on recombinant SP-C.[19,45−47] The hydrophobicity of Hel 13-5 was estimated both theoretically and experimentally. Although rSP-C forms a transmembrane α-helix across the air−water interface, Hel 13-5 and KL_4 take amphiphilic α-helical structures at the interface. Notice that Hel 13-5 has an amphiphilic structure with a 260° hydrophobic sector region, as shown in helical wheel representations (Figure 1b), when it forms an ideal α-helical structure. It means that the hydrophobic part and the hydrophilic one are completely divided into two regions in the α-helical structure, in contrast to those of KL_4 and rSP-C. This complete separation enhances the interfacial functions of Hel 13-5.[35,36]

To better understand the effects of each component in monolayer states, the phase behavior of pure DPPC, Hel 13-5 monolayers, and model surfactant lipids [DPPC/egg-PG (68:22, by weight) and DPPC/PA (90:9, by weight)] was investigated

(39) Flanders, B. N.; Vickery, S. A.; Dunn, R. C. *J. Phys. Chem. B* **2002**, *106*, 3530−3533.
(40) Koppenol, S.; Tsao, F. H. C.; Yu, H.; Zografi, G. *Biochim. Biophys. Acta* **1998**, *1369*, 221−232.
(41) Lipp, M. M.; Lee, K. Y. C.; Waring, A.; Zasadzinski, J. A. *Biophys. J.* **1997**, *72*, 2783−2804.
(42) Courrier, H. M.; Vandamme, T. F.; Krafft, M. P.; Nakamura, S.; Shibata, O. *Colloids Surf., A* **2003**, *215*, 33−41.
(43) Hiranita, T.; Nakamura, S.; Kawachi, M.; Courrier, H. M.; Vandamme, T. F.; Krafft, M. P.; Shibata, O. *J. Colloid Interface Sci.* **2003**, *265*, 83−92.
(44) Nakahara, H.; Nakamura, S.; Kawasaki, H.; Shibata, O. *Colloids Surf., B* **2005**, *41*, 285−298.
(45) Amrein, M.; Nahmen, A. V.; Sieber, M. *Eur. Biophys. J.* **1997**, *26*, 349−357.
(46) Grigoriev, D. O.; Krägel, J.; Akentiev, A. V.; Noskov, B. A.; Miller, R.; Pison, U. *Biophys. Chem.* **2003**, *104*, 633−642.
(47) Krol, S.; Ross, M.; Sieber, M.; Künneke, S.; Galla, H.-J.; Janshoff, A. *Biophys. J.* **2000**, *79*, 904−918.

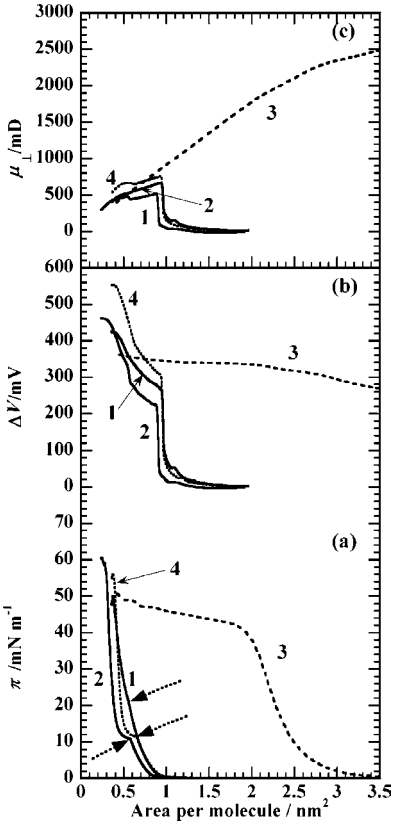

Figure 2. (a) $\pi-A$ isotherms, (b) $\Delta V-A$ isotherms, and (c) $\mu_\perp-A$ isotherms of (1) DPPC/egg-PG (68:22, wt/wt), (2) DPPC/PA (90:9, wt/wt), (3) pure Hel 13-5, and (4) pure DPPC monolayers on a 0.02 M Tris buffer solution (pH 8.4) with 0.13 M NaCl at 298.2 K.

first. The lipid mixture (DPPC/PG/PA = 68:22:9, by weight) has been shown to be the composition most similar to alveolar membranes.[28,37−38] Figure 2 showed the isotherm data from $\pi-A$, $\Delta V-A$, and $\mu_\perp-A$ measurements of these monolayers spread on a 0.02 M Tris buffer solution (pH 8.4) with 0.13 M NaCl at 298.2 K. The vertical component of surface dipole moments, $\mu_\perp$, was obtained by calculating from the Helmholtz equation:

$$\Delta V = \mu_\perp/\epsilon_0\epsilon A \qquad (1)$$

where ϵ_0 is a permittivity of a vacuum and ϵ is the mean permittivity of monolayers (which is assumed to be 1). A transition pressure and collapse pressure are generally determined only from $\pi-A$ isotherms. However, it can be more precisely decided by using $\Delta V-A$ and $\mu_\perp-A$ isotherms, as reported previously.[36] A pure DPPC monolayer has a kink point corresponding to liquid-expanded (LE)/LC coexistence states, indicated by dashed arrows in Figure 2a. The transition point appeared at 11.3 mN m^{-1} (0.65 nm^2). Monolayer collapse pressures mean maximum surface pressures, or minimum surface tensions, where conversions of monolayer states (two-dimensional (2-D) phases) to other states (three-dimensional (3-D) phases: bilayer, multilayer, folding, etc.) begin to take place. For DPPC, its collapse pressure is 55.4 mN m^{-1} (0.34 nm^2). These values show good agreement with previous papers.[36,44,48−51] In the DPPC/egg-PG and DPPC/PA monolayers, the LE/LC transition occurs at 21.8 mN m^{-1} (0.56 nm^2) and 10.8 mN m^{-1} (0.58 nm^2), respectively. Furthermore, the DPPC/egg-PG mixture reaches the collapse point at 45.4 mN m^{-1} (0.40 nm^2), and the DPPC/PA mixture reaches it at 59.7 mN m^{-1} (0.28 nm^2). The DPPC/egg-PG mixture indicates a phase separation pattern, whereas the DPPC/PA mixture indicates miscible patterns in the monolayer state, because pure DPPC, egg-PG (not shown), and PA (not shown) monolayers reflect LC, LE, and LC phases, respectively, at the high-pressure range under these experimental conditions. Therefore, the $\pi-A$ isotherm for Hel 13-5 alone appears to be stable up to ∼42 mN m^{-1} of its collapse pressure. Hel 13-5 has no first-order transition point, and its $\pi-A$ isotherm is more expanded, indicating the formation of homogeneous disordered phases over all surface pressures. This is supported morphologically in the latter section of the FM. An extrapolated area of Hel 13-5 in the condensed state is ∼2.6 nm^2, where an entire surface is covered with Hel 13-5 molecules. Beyond ∼42 mN m^{-1}, the Hel 13-5 monolayer begins to transform into 3-D reservoirs.[36]

The surface potentials (ΔV), which generally provide information about the orientation of the monolayers of DPPC, Hel 13-5, DPPC/egg-PG, and DPPC/PA, always show large positive variations under compression (Figure 2b). Some kink points corresponding to phase transitions appear on $\Delta V-A$ isotherms more clearly, revealing that ΔV is more sensitive to phase changes than π. The ΔV value of pure DPPC increases from ∼0 to ∼550 mV with decreasing surface area, indicating good agreement with previous papers.[35,36,50−52] The ΔV values of DPPC/egg-PG and DPPC/PA also increase from ∼0 to ∼420 mV and from ∼0 to ∼460 mV, respectively. In addition, these model mixtures consist mainly of DPPC, and, therefore, the features of $\Delta V-A$ isotherms for them show a similar shape (sharp jumps, etc.). On the other hand, the $\Delta V-$A isotherm of Hel 13-5 demonstrates the different behavior and profile. It slowly and monotonically increases up to ∼380 mV under compression (Figure 2b), indicating that Hel 13-5 forms a typical disordered film.

The variation in the vertical components of the surface dipole moment ($\mu_\perp$) for these monolayers upon compression is shown in Figure 2c. The $\mu_\perp$ value strongly depends on the nature of the tail group, the polar headgroups, and the subphase. Under compression from 1.00 to 0.20 nm^2, the $\mu_\perp-A$ isotherm of pure DPPC decreases to ∼500 mD, whereas that of DPPC/egg-PG and DPPC/PA monotonically decreases to ∼400 and ∼300 mD, respectively. In contrast, that of Hel 13-5 monotonically decreases to ∼400 mD from the large area to the small area.

It is widely accepted that fluorescent probes are selectively dissolved in LE phases and not in LC phases. Therefore, LC domains can be visualized as dark domains in the LE/LC coexistence region. Figure 3 shows a series of fluorescent images of DPPC/egg-PG, DPPC/PA, and pure Hel 13-5 monolayers at various surface pressures. First, in the DPPC/egg-PG films (Figure 3a), the homogeneous LE phase is indicated at 20 mN m^{-1}, and the LE/LC coexistence state is reached at 25 and 30 mN m^{-1}, where bright regions and dark domains (indicated by arrows) represent the LE and LC phases, respectively. The phase separation (the LE/LC coexistence state) is continuously observed beyond 30 mN m^{-1} up to its collapse pressure (∼45 mN m^{-1}). Second, the DPPC/PA films (Figure 3b) display the LE phase at 10 mN m^{-1}. Upon further compression, the films start to change the phase state from LE to LC phases at 10.8 mN m^{-1}. In comparison with LC domains of pure DPPC monolayers in the previous data,[36] bigger LC domains appear, resulting from a reduction in the line tensions and from an improvement in

(48) Romão, R. I. S.; da Silva, A. M. G. *Chem. Phys. Lipids* **2004**, *131*, 27−39.
(49) Gong, K.; Feng, S.-S.; Go, M. L.; Soew, P. H. *Colloids Surf., A* **2002**, *207*, 113−125.
(50) Nakahara, H.; Nakamura, S.; Nakamura, K.; Inagaki, M.; Aso, M.; Higuchi, R.; Shibata, O. *Colloids Surf., B* **2005**, *42*, 157−174.
(51) Nakahara, H.; Nakamura, S.; Nakamura, K.; Inagaki, M.; Aso, M.; Higuchi, R.; Shibata, O. *Colloids Surf., B* **2005**, *42*, 175−185.
(52) Diociaiuti, M.; Ruspantini, I.; Giordani, C.; Bordi, F.; Chistolini, P. *Biophys. J.* **2004**, *86*, 321−328.

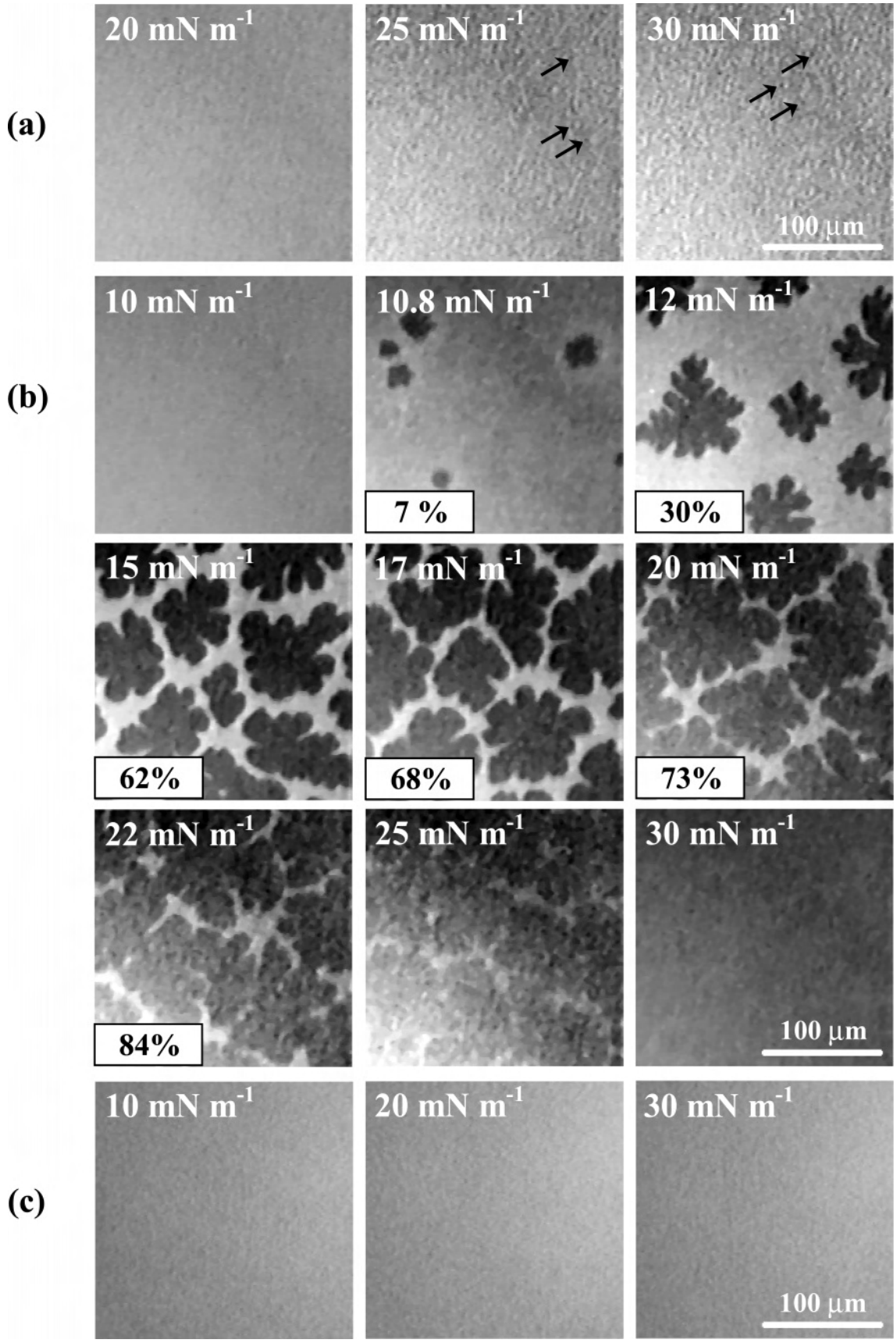

Figure 3. Fluorescent micrographs of (a) DPPC/egg-PG (68:22, wt/wt), (b) DPPC/PA (90:9, wt/wt), and (c) pure Hel 13-5 at various surface pressures. In the presence of two phases, the percentage refers to the LC phase (or ordered domains) in the micrograph. The monolayers contain 1 mol % of fluorescent probe (R18). The scale bar in the lower right represents 100 μm.

molecular packing by adding small amounts of PA molecules. The LE/LC coexistence state appears from 10.8 to 22 mN m^{-1}, and the LC domains grow larger and larger upon compression; the ratio (percentage) of LC domains per each frame increases (7, 30, 62, 68, 73, and 84%), in turn. At 25 mN m^{-1}, the image represents the LE/LC coexistence state, where almost the entire

area is occupied by the LC phase. The complete LC phase appears at 30 mN m^{-1}. When the films are compressed further, they continued to provide dark homogeneous images of the LC phase up to its collapse pressure (~60 mN m^{-1}). There are clear differences between the two model surfactant mixtures in the fluorescent micrographs. The DPPC/egg-PG monolayer shows phase separation types (Figure 3a), whereas the DPPC/PA monolayer indicates miscible types from low surface pressure to high surface pressure (Figure 3b). Third, in pure Hel 13-5 films (Figure 3c), bright homogeneous images are continuously observed up to its collapse pressure (~42 mN m^{-1}), providing evidence that Hel 13-5 forms the typical disordered film.

Ternary Systems of Model Surfactant Lipid and Hel 13-5. Typical isotherms for the fixed composition of DPPC/egg-PG (68/22, by weight) and DPPC/PA (90/9, by weight) systems with Hel 13-5 peptides have been investigated to assess each role of the PG and PA components in the ternary systems. For this purpose, the $\pi-A$, $\Delta V-$A, and $\mu_{\perp}-A$ isotherms of the three-component monolayers were measured at various Hel 13-5 molar fractions ($X_{\text{Hel 13–5}}$) on 0.02 M Tris buffer (pH 8.4) with 0.13 M NaCl at 298.2 K. The isotherms of two systems at discrete molar fractions are also inserted in the corresponding Figure 4A−B′.

For all of the molar regions of Hel 13-5 in Figure 4A,B, both of the ternary systems indicate a similar behavior in that all of the isotherms exist between those of the model lipids and pure Hel 13-5 and that they successively change with $X_{\text{Hel 13–5}}$. In particular, the $\pi-A$ isotherms at $X_{\text{Hel 13–5}} > 0.1$ of both systems show almost the same behavior as those of pure Hel 13-5 monolayers. In both systems, the specific behavior of the appearance of plateau regions on $\pi-A$ isotherms at ~42 mN m^{-1} is observed. Natural PS consists of only ~5 wt % surfactant proteins, and therefore it is necessary to examine smaller molar regions of Hel 13-5, as shown Figure 4A′,B′.

For the DPPC/egg-PG/Hel 13-5 system, as shown in Figure 4A′, the $\pi-A$ isotherms exhibit two plateau regions (or two kink points) at ~21 and ~42 mN m^{-1}; they are indicated by arrows at representative $X_{\text{Hel 13–5}} = 0.1$ (curve f). The first plateau at low surface pressure and the second plateau at high surface pressure appear as a result of the first-order−disorder/order transition and the collapse of the Hel 13-5 monolayer, respectively, whereas all of the $\pi-A$ isotherms at $X_{\text{Hel 13–5}} > 0.05$ possess only the first plateau. All of the $\pi-A$ isotherms have the first plateaus at the same surface pressure (transition pressure, $\pi^{\text{eq}} = \sim 21$ mN m^{-1}), and the kink points become unclear with increasing $X_{\text{Hel 13–5}}$. The second kink point at $X_{\text{Hel 13–5}} = 0.1$ appears at ~42 mN m^{-1} (or the collapse pressure of Hel 13-5), and the second plateau range expands as the amount of Hel 13-5 increases (Figure 4A). The DPPC/egg-PG monolayer forms a stable film up to ~45 mN m^{-1}. On the other hand, the ternary DPPC/egg-PG/Hel 13-5 monolayers ($0 < X_{\text{Hel 13–5}} \leq 0.1$) can retain stable states up to ~55 mN m^{-1} (see the inset in Figure 4A′). This is the first evidence that Hel 13-5 attractively interacts with the fluid component (egg-PG), and the two fluid components begin to be squeezed out of the ternary mixtures at ~42 mN m^{-1}. Then the degree of squeezing-out is gradually enhanced upon further compression, and the interface is ultimately refined to DPPC-rich monolayers at ~55 mN m^{-1} because the collapse pressure of the DPPC monolayers is ~55 mN m^{-1} (Figure 2A). At ~42 mN m^{-1}, the $\Delta V-A$ isotherm in $X_{\text{Hel 13–5}} = 0.1$ shows a kink point corresponding to the second plateau on its $\pi-A$ isotherm, as indicated by an arrow, and then the ΔV value gradually rises upon further compression, indicating that monolayer orientations change due to the exclusion of fluid materials. Finally, it becomes constant above 55 mN m^{-1}. This also supports the squeeze-out phenomenon of Hel 13-5.

For the DPPC/PA/Hel 13-5 system shown in Figure 4B′, $\pi-A$ isotherms also have two plateau regions at ~10−14 mN m^{-1} and ~42 mN m^{-1}. The $\pi-A$ isotherm at $X_{\text{Hel 13–5}} = 0.005$ has only the first plateau. On the other hand, two plateaus are observed in the $\pi-A$ isotherms of $0.01 < X_{\text{Hel 13–5}} < 0.1$. Their transition pressures of the first plateau change from 10.9 to 13.7 mN m^{-1} (Figure 4B′) and become unclear with increasing $X_{\text{Hel 13–5}}$, which is the same as the DPPC/egg-PG/Hel 13-5 system. The second kink points in $0.01 < X_{\text{Hel 13–5}} < 0.1$ also appear at ~42 mN m^{-1}, and the second plateau range elongates as the amount of Hel 13-5 increases (Figure 4B,B′). This behavior is the same as that of the DPPC/egg-PG/Hel 13-5 system. However, the DPPC/PA/Hel 13-5 system displays a more jagged second plateau, revealing that the Hel 13-5 species is not easily squeezed out of the ternary monolayers because of the absence of fluid components. In contrast to the collapse behavior of the DPPC/egg-PG/Hel 13-5 system, the DPPC/PA monolayer forms a stable film up to ~60 mN m^{-1}, and all of the DPPC/PA/Hel 13-5 monolayers ($0 < X_{\text{Hel 13–5}} < 0.1$) also remain stable up to ~60 mN m^{-1}, despite adding Hel 13-5 to the DPPC/PA monolayer (see the inset in Figure 4B′). This also reveals that Hel 13-5 interacts with rigid components (DPPC and PA), even at high surface pressures, and only Hel 13-5 is gradually squeezed out of the ternary monolayers above ~42 mN m^{-1}. That is, the squeezing-out manages to gradually start upon further compression, and the interface becomes rich in the DPPC/PA monolayer at ~60 mN m^{-1}. At >42 mN m^{-1}, the $\Delta V-A$ isotherms within $0.01 < X_{\text{Hel 13–5}} < 0.1$ indicate the same behavior as that of the above-mentioned DPPC/egg-PG/Hel 13-5 system.

Analysis by Additivity Rule. A better understanding of the interactions between the lipids and Hel 13-5 is provided by examining whether mean molecular areas as a function of $X_{\text{Hel 13–5}}$ satisfy the additivity rule.[53,54] A comparison between the experimental mean molecular areas (solid points) and the mean molecular areas (dashed lines) of an ideal mixing[15−17] is shown in Figure 5 at four different surface pressures (5, 15, 25, and 35 mN m^{-1}). Both the ternary systems show good linearity and agreement with the ideal line at all surface pressures, implying complete phase separations or complete miscible patterns. Considering the later-mentioned fluorescent micrographs (Figure 8), both of these monolayers support the former.

Surface potential measurements provide sensitive responses to the variation in the molecular packing and orientation. The surface potential (ΔV) of the monolayer is also analyzed in terms of the additivity rule at the four pressures. For both ternary systems, the experimental ΔV is presented by the solid points in Figure 6, where the dashed lines show the ΔV calculated by assuming the additivity rule.[53,54] In the DPPC/egg-PG/Hel 13-5 mixture (Figure 6a), positive deviations ($0.005 < X_{\text{Hel 13–5}} < 0.3$) and negative ones ($X_{\text{Hel 13–5}} = 0.4$ and 0.7) from ideal lines are observed at all surface pressures. In addition, it will be divided into two parts by the transition pressure (π^{eq}) of the DPPC/egg-PG system ($\pi^{\text{eq}} = \sim 20$ mN m^{-1}); one is the lower surface pressure part (the 5 and 15 mN m^{-1} group) and the other is the higher one (the 25 and 35 mN m^{-1} group). Concerning the slope of the ideal line, the former is positive and the later is negative. The $\Delta V-X_{\text{Hel 13–5}}$ at smaller molar fractions ($0.005 < X_{\text{Hel 13–5}} < 0.3$) displays a specific behavior, indicating that the addition of a small amount of Hel 13-5 enhances the vertical orientation of two tilted acyl chains of DPPC monolayers, where the chain

(53) Marsden, J.; Schulman, J. H. *Trans. Faraday Soc.* **1938**, *34*, 748−758.
(54) Shah, D. O.; Schulman, J. H. *J. Lipid Res.* **1967**, *8*, 215−226.

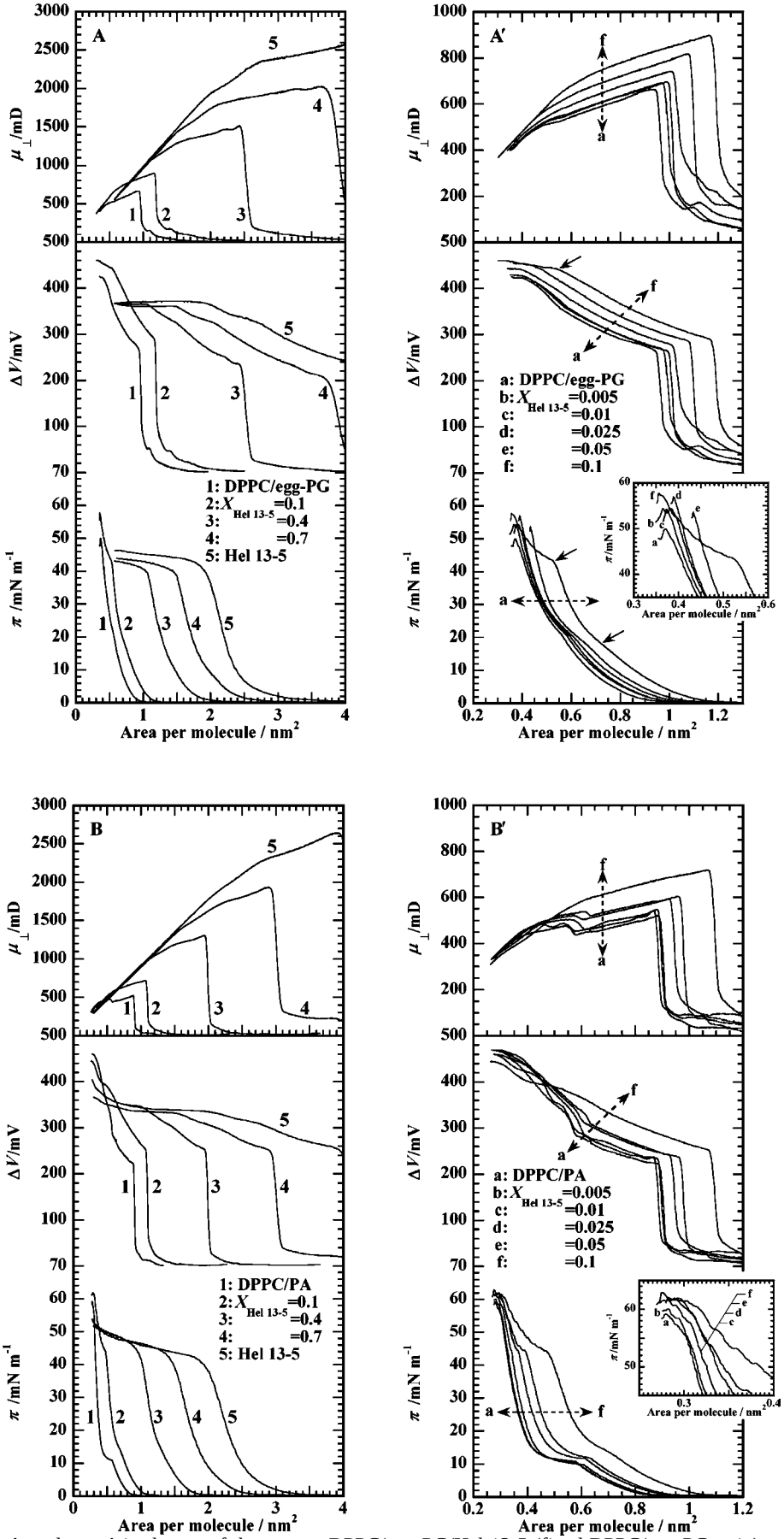

Figure 4. $\pi-A$, $\Delta V-A$, and $\mu_{\perp}-A$ isotherms of the ternary DPPC/egg-PG/Hel 13-5 (fixed DPPC/egg-PG ratio) and DPPC/PA/Hel 13-5 (fixed DPPC/PA ratio) mixtures on a 0.02 M Tris buffer solution (pH 8.4) with 0.13 M NaCl at 298.2 K. (A) DPPC/egg-PG/Hel 13-5 (A′: $0 \le X_{\text{Hel 13-5}} \le 0.1$), (B) DPPC/PA/Hel 13-5 (B′: $0 \le X_{\text{Hel 13-5}} \le 0.1$). (Inset) Enlarged $\pi-A$ isotherms at high surface pressures (A′ and B′).

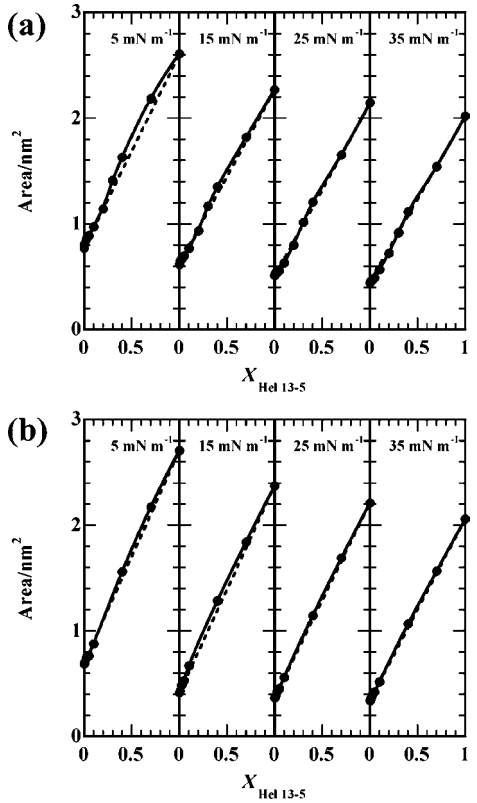

Figure 5. Mean molecular area (A) of (a) DPPC/egg-PG/Hel 13-5 and (b) DPPC/PA/Hel 13-5 mixtures as a function of $X_{\text{Hel 13-5}}$ at four different pressures. The dashed lines were calculated by assuming the additivity rule, and the solid points represent experimental values.

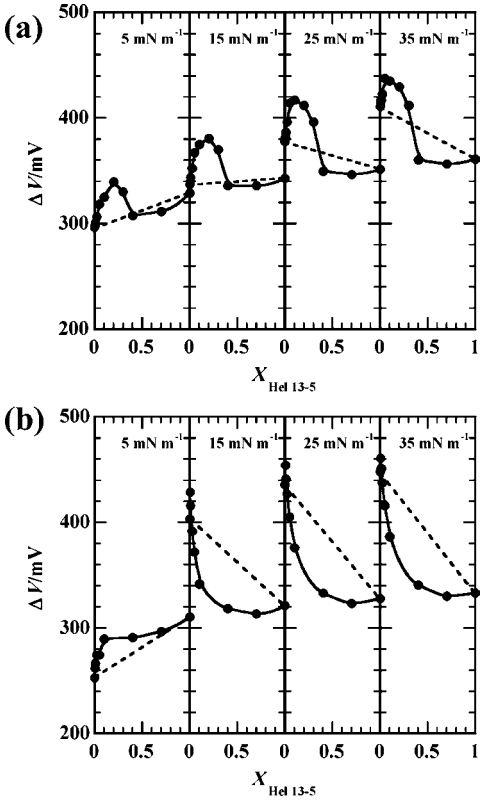

Figure 6. Surface potential (ΔV) of the (a) DPPC/egg-PG/Hel 13-5 and (b) DPPC/PA/Hel 13-5 mixtures as a function of $X_{\text{Hel 13-5}}$ at four different pressures. The dashed lines were calculated by assuming the additivity rule, and the solid points represent experimental values.

length distribution and the double bond of egg-PG seem to contribute to their easy packing at smaller molar fractions ($0.005 < X_{\text{Hel 13-5}} < 0.3$). However, the $\Delta V - X_{\text{Hel 13-5}}$ at larger molar fractions ($X_{\text{Hel 13-5}} = 0.4$ and 0.7) shows almost the same ΔV value as that of pure Hel 13-5. This implies that the surface potential behavior is governed by the large amount of Hel 13-5 with little contributions from the DPPC/egg-PG components.

For the DPPC/PA/Hel 13-5 system, the positive deviation part ($0.005 < X_{\text{Hel 13-5}} < 0.5$) and the good agreement part ($X_{\text{Hel 13-5}} = 0.7$) at 5 mN m^{-1} are observed in Figure 6b, whereas the $\Delta V - X_{\text{Hel 13-5}}$ at 15−35 mN m^{-1} shows the positive deviation parts at $X_{\text{Hel 13-5}} = 0.005$ and 0.01 and the negative ones at $0.025 < X_{\text{Hel 13-5}} < 0.7$. In this case, it will be also divided into two parts by the transition pressure (π^{eq}) of the DPPC/PA system ($\pi^{\text{eq}} = \sim 10$ mN m^{-1}): one being the lower surface pressure part (the 5 mN m^{-1} group), and the other being the higher one (the 15, 25, and 35 mN m^{-1} one). Concerning the slope of the ideal line, the former is positive, and the later is negative. Similar to the DPPC/egg-PG/Hel 13-5 system, the $\Delta V - X_{\text{Hel 13-5}}$ in the smaller $X_{\text{Hel 13-5}}$ also exhibits a specific behavior for the DPPC/PA/Hel 13-5 system. Especially at $X_{\text{Hel 13-5}} = 0.005$ and 0.01, ΔV is dramatically increased compared with the ideal line. This behavior is also the case for the DPPC/Hel 13-5 binary system,[36] where the additivity relationship of $\Delta V - X_{\text{Hel 13-5}}$ shows negative deviation from the ideal line, except for $X_{\text{Hel 13-5}} = 0.1-0.2$ at 5 mN m^{-1}. On the contrary, the DPPC/PA/Hel 13-5 system shows a positive deviation, where PA acts like a filler to promote more compact packing in the monolayer state. In larger $X_{\text{Hel 13-5}}$, however, the additivity relationship of $\Delta V - X_{\text{Hel 13-5}}$ shows negative deviation from the ideal line, and the ΔV value is also similar to that of pure Hel 13-5 for the DPPC/PA/Hel 13-5 system. These results reveal that the addition of just a small amount of Hel 13-5 dramatically generates the driving force of the squeeze-out.[36]

The interfacial behavior of PS has been enthusiastically investigated by many researchers. However, few analyses using surface potential data have been employed.[55,56] PS functionally works at and through the air−water interface. In the vicinity of the interface, they indicate various conformations with breath movements. In a previous study,[36] the authors showed the specific deviations from the ideal lines for surface potentials in the binary DPPC/Hel 13-5 system relative to the additivity of the surface potential. These deviations suggested that the monolayer orientation of our synthetic pulmonary preparations varied from low surface pressure to the onset of the squeeze-out of Hel 13-5. In the present study, such behavior was also observed in both of the ternary systems (Figure 6). We used two model surfactant lipids with fixed ratios: DPPC/egg-PG (= 68:22, by weight) and DPPC/PA (= 90:9, by weight) mixtures. Considering that our two model surfactant lipids contain mainly DPPC and that the ΔV value is governed by DPPC at close-packed conformation in the system, these positive deviations might contribute to the vertical orientation of the DPPC hydrophobic chains induced by the mutual interactions regarding the driving force of the squeeze-out motion.

Cyclic Compression−Expansion Isotherms. The repeated compression−expansion cycling $\pi - A$ and $\Delta V - A$ isotherms[55,57−58] (known as hysteresis curves) of ternary DPPC/egg-PG/Hel 13-5

(55) Watkins, J. C. *Biochim. Biophys. Acta* **1968**, *152*, 293−306.
(56) Discher, B. M.; Maloney, K. M.; Grainger, D. W.; Hall, S. B. *Biophys. Chem.* **2002**, *101−102*, 333−345.
(57) Galdston, M.; Shah, D. O.; Shinowara, G. Y. *J. Colloid Interface Sci.* **1969**, 29, 319−334.
(58) Petrov, O. V. *Bull. Exp. Biol. Med.* **1974**, *77*, 210−212.

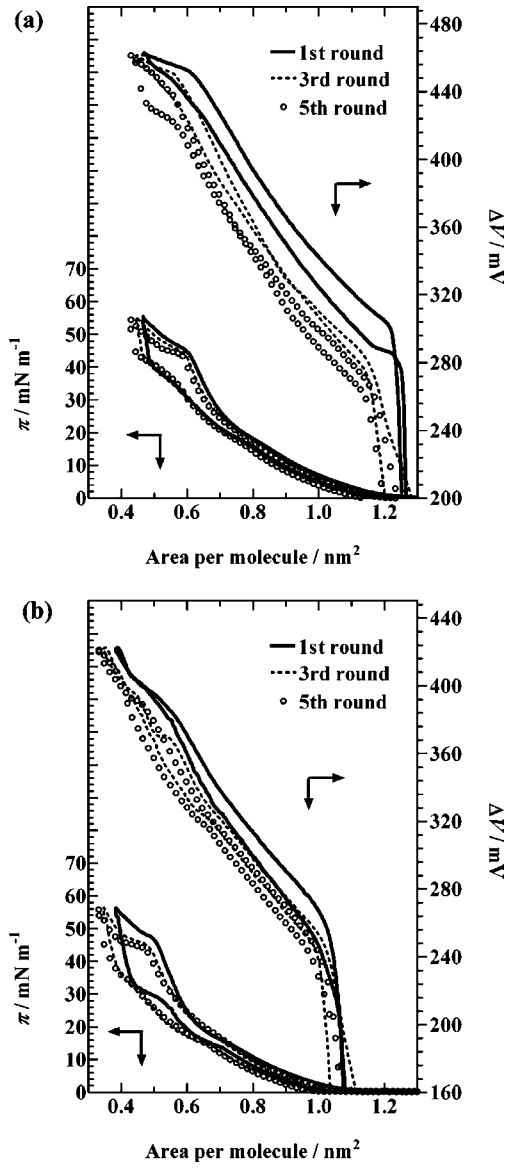

Figure 7. Cyclic compression and expansion isotherms (or hysteresis curves) of the (a) DPPC/egg-PG/Hel 13-5 and (b) DPPC/PA/Hel 13-5 mixtures at $X_{\text{Hel }13-5} = 0.1$ on a 0.02 M Tris buffer solution (pH 8.4) with 0.13 M NaCl at 298.2 K. The compression and expansion cycle was performed five times at the compression rate of ~0.1 nm^2 molecule^{-1} min^{-1}.

(a) and DPPC/PA/Hel 13-5 (b) systems at $X_{\text{Hel }13-5} = 0.1$ are shown for the first, third, and fifth rounds in Figure 7. These two systems were compressed up to a surface pressure of ~55 mN m^{-1} and then expanded to the respective starting area. In Figure 7a, the second kink point clearly appears, despite the repeated cycling processes, indicating that Hel 13-5 is reversibly desorbed into the subphase in both the $\pi-A$ and $\Delta V-A$ isotherms. Concerning the $\Delta V-A$ isotherms in the fifth round of the expansion process, it is clear that surface potential drops of ~30 mV occurred. That means that DPPC and egg-PG interaction is not very strong because of the different type of phase behaviors between the liquid expanded film of egg-PG and the LE/LC type of DPPC. In Figure 7b, for $\pi-A$ isotherms, the second kink shoulder for repeated hysteresis curves clearly appears without becoming unclear as it does in Figure 7a. For the first, third, and fifth rounds in the $\Delta V-A$ isotherms, compression and expansion processes are almost the same in the range from about 0.35 to 0.50 nm^2, although the area is shifted to a small area. This behavior may deduce that the addition of PA to a DPPC monolayer led to a better ordered monolayer, and PA leads to a reduction in the tilt angle of the aliphatic chains of DPPC.[59] As for the $\pi-A$ isotherms, surface pressure decreases sharply like a solid film in the expansion process.

Consequently, Figure 7 indicates good respreading behavior from the first to fifth rounds, showing the ability of the desorbed molecules to come back into the interface. These results demonstrate that small amounts of Hel 13-5 peptides can accelerate the good respreading of rigid components (DPPC and PA).

Fluorescence Microscopy. An FM observation was carried out to know the morphological effects of Hel 13-5 on binary DPPC/PA monolayers. Figure 8 shows FM images of ternary DPPC/PA/Hel 13-5 monolayers at $X_{\text{Hel }13-5} = 0.01$. Two-phase coexistence states similar to the resultant images in the DPPC/PA monolayer system (see Figure 3b) are also clearly observed. They indicate a homogeneous disordered phase at 10 mN m^{-1} and disorder/order coexistence phases at 15−30 mN m^{-1}. However, the image at 30 mN m^{-1} displays an almost ordered phase. With increasing surface pressure from 15 to 20 mN m^{-1}, ordered domains grow larger: the ordered percentage increases from 57 to 65%. The micrographs at 35 and 40 mN m^{-1} show the dark homogeneous images. Once the micrographs became dark homogeneously, the dark images remained, as is the case in the DPPC/PA system. Generally, aggregations of fluorescent probes induce a self-quenching, and the probe cannot emit fluorescence. From the image at 45−55 mN m^{-1}, the micrographs are released from quenching, and the contrast becomes gradually clearer. It is clearly shown that this specific behavior reflects the squeeze-out of Hel 13-5 between 40 and 45 mN m^{-1}. In addition, the micrographs at 20 and 55 mN m^{-1} have the same ordered domains in size. However, smaller disordered regions are observed in the FM image at 55 mN m^{-1}; ordered domains in the image at 55 mN m^{-1} are more packed, supporting the squeeze-out of Hel 13-5.

Discussion

The squeeze-out theory has been confirmed using various experimental techniques such as Langmuir isotherms,[15−17] microscopy,[20,60] spectroscopy,[61] and X-ray diffractions.[62] It means that complete phase separations of the rigid from the fluid components take place in multicomponent monolayers, and selective exclusions of the fluid components occur at the collapse pressure of the fluid proteins. In general, squeezed-out materials are reincorporated into the monolayer upon expansion. However, the theory has not provided an explanation of squeeze-out mechanisms. The addition of small amounts of proteins (peptides) gives rise to a driving force for squeeze-out events. Krol and co-workers[47] reported that two plateau regions were observed on the $\pi-A$ isotherm for the DPPC/dipalmitoyl-PG (DPPG) (4:1, by molar ratio) plus 1% SP-B system and that the appearance of the second plateau region at ~40 mN m^{-1} was independent of SP-B content, and its plateau became wide as the amount of SP-B increased. Generally, the appearance of a second plateau corresponding to the collapse pressure of the proteins or peptides reflects squeeze-out events and is significant to prevent alveoli from collapsing during respiration. In the present study, when

(59) Lee, K. Y. C.; Gopal, A.; Nahmen, A. V.; Zasadzinski, J. A.; Majewski, J.; Smith, G. S.; Howes, P. B.; Kjaer, K. *J. Chem. Phys.* **2002**, *116*, 774−783.
(60) Piknova, B.; Schief, W. R.; Vogel, V.; Discher, B. M.; Hall, S. B. *Biophys. J.* **2001**, *81*, 2172−2180.
(61) Brockman, J. M.; Wang, Z.; Notter, R. H.; Dluhy, R. A. *Biophys. J.* **2003**, *84*, 326−340.
(62) Alonso, C.; Alig, T.; Yoon, J.; Bringezu, F.; Warriner, H.; Zasadzinski, J. A. *Biophys. J.* **2004**, *87*, 4188−4202.

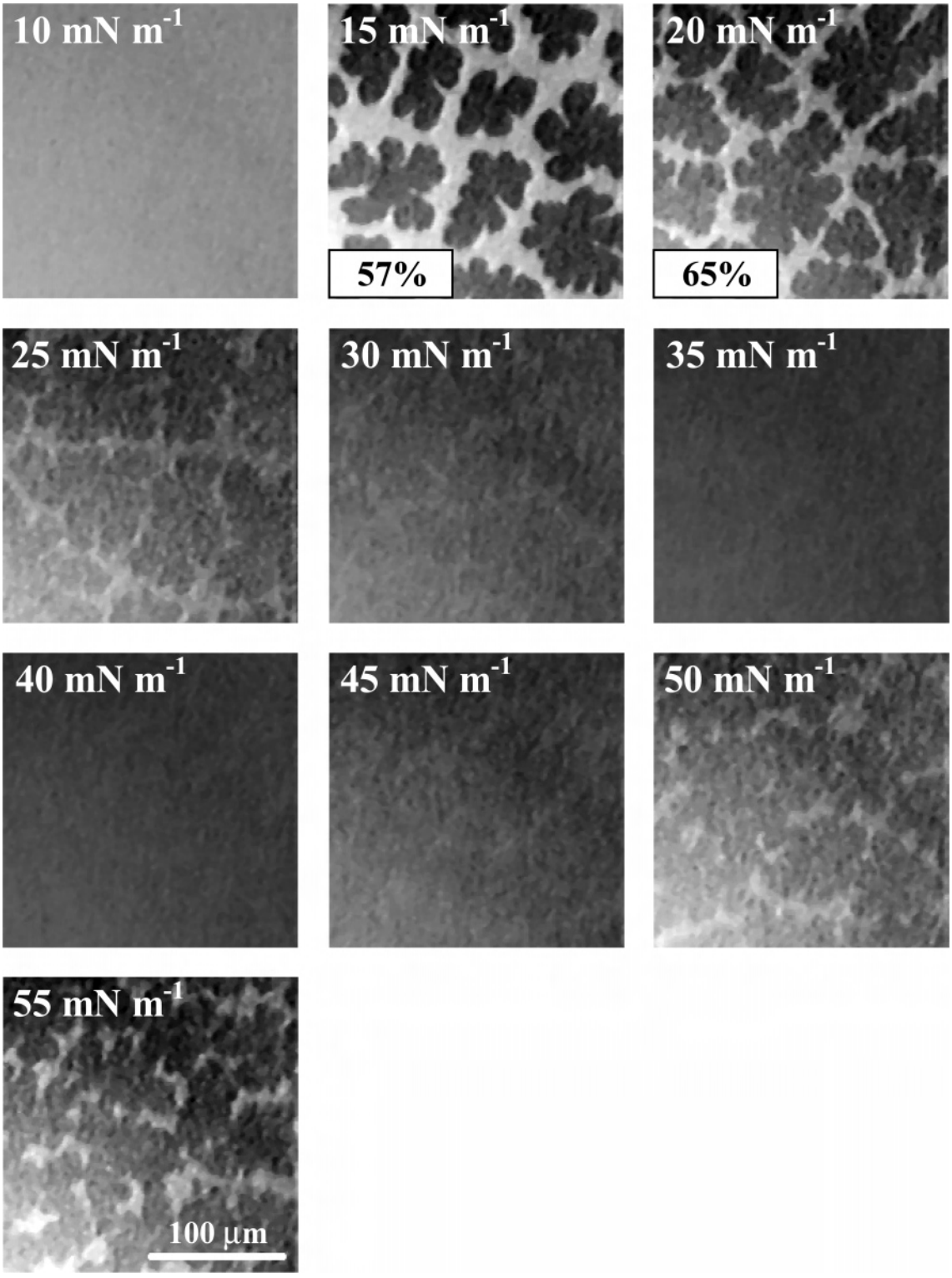

Figure 8. Fluorescent micrographs of the DPPC/PA/Hel 13-5 mixture system at $X_{\text{Hel 13-5}} = 0.01$ from $\pi = 10-55$ mN m^{-1}. In the coexistence phase, the percentage refers to ordered domains in the micrograph. The monolayers contain 1 mol % of fluorescent probe (R18). The scale bar in the lower right represents 100 μm.

a small amount of Hel 13-5 is added to the two model surfactant lipids, such plateaus also appear at 42 mN m^{-1} (Figure 4). This implies a similarity in the surface activities between Hel 13-5 and SP-B.

Some articles about the role of palmitoyloleoyl-PG (POPG) and proteins in ternary DPPC/POPG/protein monolayers have been reported.[63,64] POPG is a major unsaturated anionic component in egg-PG molecules and generally forms a stable LE film. It is also known to spread relatively rapidly at the air−water interface. Negatively charged POPG selectively interacts with positively charged SP-B and -C by an electrostatic attraction and an LE−LE miscibility. Therefore, these proteins

(63) Nag, K.; Munro, J. G.; Inchley, K.; Schürch, S.; Petersen, N. O.; Possmayer, F. *Am. J. Physiol.* **1999**, *277*, L1179−L1189.
(64) Putz, G.; Walch, M.; Eijk, M. V.; Haagsman, H. P. *Biochim. Biophys. Acta* **1999**, *1453*, 126−134.

are preferentially squeezed out with POPG molecules from multicomponent systems, facilitating the formation of stable 3-D aggregates.[22] For the ternary DPPC/egg-PG/Hel 13-5 system (Figure 4A′), the second collapse pressures (π^c) of ~55 mN m^{-1} at smaller $X_{\text{Hel 13-5}}$ (= 0.005−0.1) also indicate that the squeeze-out of Hel 13-5 with egg-PG promotes a refining of the interface to become a DPPC-rich monolayer. It was reported that only Hel 13-5 was squeezed out of the binary DPPC/Hel 13-5 system.[36] In comparison with the previous data, egg-PG was found to help Hel 13-5 molecules squeeze out of the synthetic PS monolayer, and then egg-PG and Hel 13-5 occupy 3-D surface-associated aggregates (or reservoirs).[20,36]

A few reports about the contributions of PA and proteins in the binary PA/protein system have been published.[39,41] Lee and co-workers[59] reported that, in binary DPPC/PA monolayers without proteins, the addition of PA to DPPC monolayers led to a change from a tilted to an untilted molecular packing or a better ordered monolayer. As far as we know, there is no paper that provides an interpretation of the effects of PA in the ternary DPPC/PA/protein system. DPPC is a major component in PS, and therefore investigating the role of PA surrounded by DPPC and proteins in the ternary system is an attractive challenge. For the ternary DPPC/PA/Hel 13-5 systems (Figure 4B′), $\pi-A$ isotherms at $X_{\text{Hel 13-5}} = 0.005-0.1$ indicate the fixed collapse point at ~60 mN m^{-1}, independent of the compositions, which coincides with that of the binary DPPC/PA mixture without Hel 13-5. This reveals that the squeeze-out behavior of Hel 13-5 only facilitates a compositional refinement from the ternary to binary monolayers at the interface. From the results of the binary DPPC/Hel 13-5 and ternary DPPC/egg-PG/Hel 13-5 and DPPC/PA/Hel 13-5 systems, the individual contributions to synthetic PS are clarified as follows: DPPC with PA especially facilitates the reduction of surface tension, and egg-PG and Hel 13-5 provide the driving force to fluidize the monolayer.

PS shows a variety of complex phenomena across the air−water interface, such as molecular adsorption−desorption, spreading−respreading, and squeeze-out, where combinations of all these processes are involved in retaining pulmonary stability in situ. Compression−expansion cyclic techniques, which simply imitate the dynamic variation of alveolar areas during breathing, can assess these phenomena in vitro. A large hysteresis area between the compression and expansion isotherms is desirable in the native pulmonary system.[65] In the native or replacement surfactant system, it is widely accepted that the unsaturated and anionic lipids are apt to act as emulsifiers and fluidizers that help the PS mixture rapidly adsorb into and respread at the alveolar air−liquid interface, and that the function of the PA molecules, such as fillers, improves the vertical molecular orientation of the tilted DPPC hydrophobic chains. In the present study, resultant hysteresis data indicate the effects of the addition of egg-PG and PA molecules to DPPC/Hel 13-5 mixtures. A better reproducibility at high surface pressure in the $\pi-A$ isotherm is observed in the DPPC/egg-PG/Hel 13-5 system, implying that the stable surface-associated reservoir consisting of egg-PG and Hel 13-5 forms under the interface at high surface pressure[36] and that these materials rapidly re-enter and respread at the interface. At the same time, larger hysteresis areas are produced in the DPPC/PA/Hel 13-5 system. This means that the addition of PA molecules into the DPPC/Hel 13-5 system induces a good molecular packing state, which is required for the native pulmonary system. DPPC monolayers have some defects in PS systems, such as slow respreading and poor molecular packing. However, PG and PA molecules in native PS systems capably compensate for these defects.[66,67] Each interfacial property of PG and PA is clearly confirmed in our synthetic surfactant systems, showing that the addition of PG and PA components for the general DPPC-based systems containing synthetic protein facilitates the functions of the replacement synthetic PS.

Scheme 1. New Concept Describing the Refluorescent Phenomenon through Self-Concentration Quenching of FM Probes Led to by the Squeeze-Out of Hel 13-5 Peptides from Monolayers at (a) at Low Surface Pressure (<25 mN m^{-1}), (b) Middle Surface Pressure (from 25 to 42 mN m^{-1}), and (c) High Surface Pressure (>42 mN m^{-1})

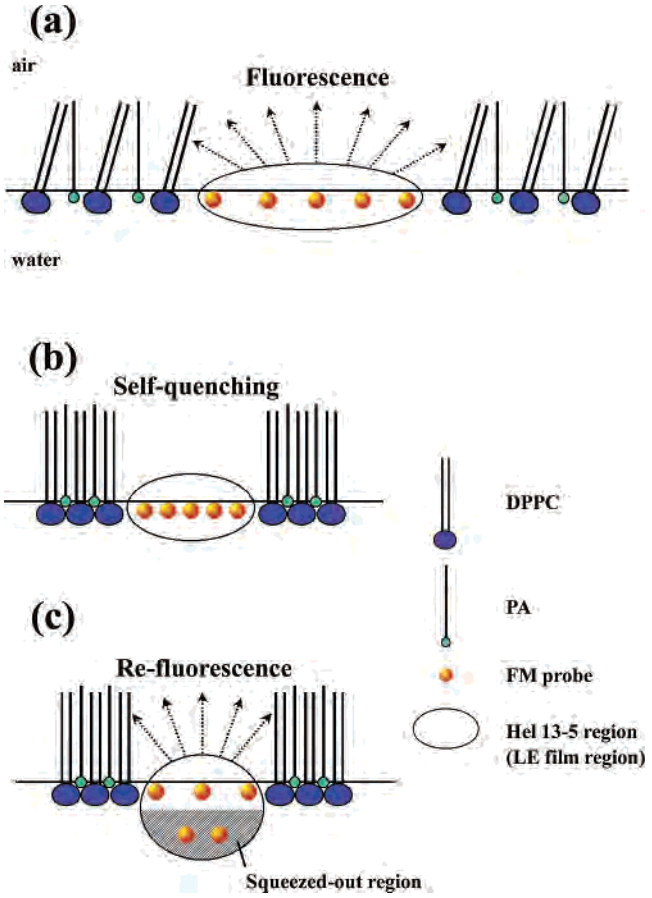

A direct imaging with FM clearly showed that the morphological behavior of the synthetic Hel 13-5 peptide and the PA molecule in the DPPC monolayer were nonideal and led to the novel morphological evidence of squeeze-out events of Hel 13-5. Aggregated fluorescent probes upon lateral compression ultimately induce self-quenching phenomena, resulting from the high probe concentration at the surface. Fluorescent probes form stable LE films and selectively dissolve in disordered lipids. Therefore, the fluorescent quenching sensitively depends on the surface quantities of such lipids. Thus, employing this quenching phenomenon can confirm the occurrence of squeeze-out phenomena from the interface. There are a few papers that interpret this behavior by applying fluorescent probe quenching. Those papers reported that, in the DPPC/DPPG/rSP-C system, clear contrast FM images of the disorder/order coexistence phase at low surface pressure were converted to unclear ones upon compression, and refluorescing images that were the same as those at low surface pressure were later observed beyond the plateau regions at high surface pressure, showing that the

(65) Banerjee, R.; Bellare, J. R. *J. Appl. Physiol.* **2001**, *90*, 1447−1454.

(66) Bringezu, F.; Ding, J.; Brezesinski, G.; Zasadzinski, J. A. *Langmuir* **2001**, *17*, 4641−4648.

(67) Cruz, A.; Vázquez, L.; Vélez, M.; Gil, J. P. *Biophys. J.* **2004**, *86*, 308−320.

fluorescent probes as well as rSP-C were excluded from the interface.[45,68] This behavior surely confirms the occurrence of squeeze-out phenomena. However, mechanisms for the restoration of the contrast of fluorescent probes during the exclusion of rSP-C peptides cannot be clarified. In this study, the molar fraction change of Hel 13-5 peptides ($X_{\text{Hel 13}-5}$) in a fixed DPPC/PA ratio or the variation of surface quantities of disordered films, in which the fluorescent probes can preferentially dissolve, provided a sharp insight into an elucidation of the mechanism for the contrast changes corresponding to squeeze-out behavior (Figure 8). In addition, the comparison between DPPC/Hel 13-5[36] and DPPC/PA/Hel 13-5 systems shows that the addition of PA into the DPPC/Hel 13-5 system effectually induces the squeeze-out behavior of Hel 13-5 because such refluorescent observations are not observed in the former system.

First, Scheme 1 shows a proposed model based on our results for the refluorescent phenomenon. FM probes emit fluorescence in a proper surface concentration (Scheme 1a). Further compression leads to a higher surface concentration, resulting in self-quenching (Scheme 1b), although it depends sensitively on the amounts of disordered films at the surface. Assuming that there are small surface quantities of Hel 13-5 ($X_{\text{Hel 13}-5} = 0.01$) at the interface, the FM images indicate complete self-quenching. On the other hand, more surface quantities ($X_{\text{Hel 13}-5} = 0.05$) induce incomplete self-quenching because of the existence of abundant disordered regions. In general, further compression causes dark homogeneous patterns in FM images. However, the squeeze-out process for Hel 13-5 peptides again recovers the coexistent images (Scheme 1c). The compression beyond the Hel 13-5 collapse pressure provides the Hel 13-5 monolayer with a driving force to squeeze out from the interface, and then a portion of the Hel 13-5 molecules is excluded into the subphase with some fluorescent probes (LE film), which is supported by atomic force microscopy (AFM) measurements in a previous study.[36] Consequently, this specific behavior also demonstrates the squeeze-out phenomenon of our synthetic peptide Hel 13-5 at the same time.

Conclusions

Langmuir isotherms reveal that the synthetic peptide Hel 13-5 with anionic egg-PG monolayers is squeezed out of the simple model system of DPPC/egg-PG/Hel 13-5, which results from the electrostatic attraction and disordered−disordered miscibility. On the other hand, they clarify the exclusion of only Hel 13-5 from the model system of DPPC/PA/Hel 13-5. It is also found that egg-PG and PA molecules work as a compensation for the functional (packing) defects of DPPC monolayers, similar to the major PS component in the synthetic replacement systems as well as native PS systems.

We have shown the first concept of the refluorescent phenomenon, which sensitively depends on the surface quantities of disordered films. Notice that the phenomenon did not occur in the binary DPPC/Hel 13-5 system in the previous study.[36] However, it occurs in the ternary DPPC/PA/Hel 13-5 system because of the good molecular-packing effects caused by the addition of PA molecules. Fluorescent probes generally form stable LE monolayers, and some of them are eliminated from the surface together with the Hel 13-5 squeezed out. This behavior leads to a weakening of the fluorescent quenching. The resultant refluorescent behavior bears out these squeeze-out events indirectly. Compared with the previous work on the simplest DPPC/Hel 13-5 system, the present work proposes the necessity of the addition of PG and PA components into synthetic replacement systems containing Hel 13-5 peptide, which can be added to make up for DPPC defects in PS functions. A thorough understanding of each role of the lipids and Hel 13-5 peptide also helps to design the replacement PS formulations containing synthetic peptides as RDS medicines. They may provide further information on the capability of surfactant replacement therapy using synthetic peptides. Our model studies are now in progress on a multicomponent DPPC/egg-PG/PA/Hel 13-5 system.

Acknowledgment. This work was supported by Grant-in-Aid for Scientific Research 17310075 from the Japan Society for the Promotion of Science and by Grant 17650139 from the Ministry of Education, Science and Culture, Japan, and by the Interchange Association, Japan, which are gratefully acknowledged. This work (H.N.) was also supported by Research Fellowships of the Japan Society for the Promotion of Science for Young Scientists (18.9587).

LA060194H

(68) Bourdos, N.; Kollmer, F.; Benninghoven, A.; Ross, M.; Sieber, M.; Galla, H.-J. *Biophys. J.* **2000**, *78*, 357−369.